

Confirmation of Anomalous Dynamical Arrest in attractive colloids: a molecular dynamics study.

E. Zaccarelli¹, G. Foffi^{1,2}, K.A. Dawson², S.V. Buldyrev³, F. Sciortino¹ and P. Tartaglia¹

¹ *Dipartimento di Fisica, Istituto Nazionale di Fisica della Materia, and INFM Center for Statistical Mechanics and Complexity, Università di Roma La Sapienza, P.le A. Moro 5, I-00185 Rome, Italy*

² *Irish Centre for Colloid Science and Biomaterials, Department of Chemistry, University College Dublin, Belfield, Dublin 4, Ireland*

³ *Center for Polymer Studies and Department of Physics, Boston University, Boston, MA 02215, USA.*
(October 30, 2018)

Previous theoretical, along with early simulation and experimental, studies have indicated that particles with a short-ranged attraction exhibit a range of new dynamical arrest phenomena. These include very pronounced reentrance in the dynamical arrest curve, a logarithmic singularity in the density correlation functions, and the existence of ‘attractive’ and ‘repulsive’ glasses. Here we carry out extensive molecular dynamics calculations on dense systems interacting via a square-well potential. This is one of the simplest systems with the required properties, and may be regarded as canonical for interpreting the phase diagram, and now also the dynamical arrest. We confirm the theoretical predictions for re-entrance, logarithmic singularity, and give the first direct evidence of the coexistence, independent of theory, of the two coexisting glasses. We now regard the previous predictions of these phenomena as having been established.

PACS numbers: 82.70Dd, 64.70Pf, 83.10Rs.

I. INTRODUCTION

Recently, there has emerged a series of remarkable results involving the dynamical arrest of particles with interaction potentials that are short compared to the size of the repulsive core [1–9]. The most important predictions are as follows [10]. The curve at which the fluid phase is arrested is reentrant in the regime where attractions and repulsions compete. In the vicinity of this reentrance, and in the arrested regime, there exists two distinct arrested states that may, under some conditions, coexist. These two states differ in their long-term dynamics. This coexistence terminates smoothly, the dynamics of the two arrested states becoming identical at a particular point at which distinctive dynamics is expected. It is important to note that all these phenomena are predicted to occur irrespective of the shape of the potential (explicit results exist for square well or hard-core Yukawa interaction models [4–7]). The essential feature is only that the range of the attraction in comparison to the hard core be extremely small.

The results described above were first deduced from the mode-coupling-theory (MCT) [11,12], and we may note that the conclusions do not depend on details of the approximation for input static structure, Percus-Yevick, Mean Spherical Approximation and Self-Consistent Ornstein-Zernike Approximation, all leading to essentially the same picture. Within MCT the merging of the two arrested states is predicted to be a higher order dynamical singularity, and density correlations in its vicinity are expected to obey a highly distinctive log-

arithmic relaxation [4,13], in contrast to the conventional ergodic-non ergodic transition where a two-step process takes place [12,14].

More recently this decay has been observed also in several experimental systems [15,16,9], thus giving the first evidence that these singularities do exist in nature.

Two recent numerical works [8,17] have focused on the new dynamical features characterizing attractive colloidal systems. In Ref. [8], colloidal interactions were modeled with a potential chosen in such a way to avoid undesired effects such as liquid-gas separation at low densities. Polydispersity was included to prevent crystallization at high densities. In Ref. [17] Molecular Dynamics simulations of a square well (SW) system with very narrow range of attraction have been performed. In both cases, the results have been shown to be in excellent agreement with MCT predictions. The focus on the simple square well potential, makes direct contact both with the available theoretical results and with experimental systems, being the interactions completely controllable and not dependent on external parameters. For the SW model, theoretical solution is also available. Indeed, the equilibrium properties of square-well potential have been studied for many years, and in many ways is regarded as the simplest physical model that exhibits all of the essential features of the short-ranged systems [18–23]. Besides this, it is the model for which the theory of the dynamical arrest transition described above has been developed [4,5] and for which, therefore, detailed comparison may be made between theory and simulation. It may therefore be regarded as canonical in this arena of study.

In Ref. [17], we examined a one-component square well

system. We found that, no matter the sharp intervening of crystallization which effectively prevented the system to approach very closely the glass transition, it was possible to have a clear picture of the reentrant shape of the glass curve in the temperature-density plane. This was achieved by plotting iso-diffusivity curves, and examining their trends when approaching the limit $D \rightarrow 0$. The shape of the liquid-glass line found was in good agreement with the previous MCT [4] predictions.

In this paper, we report an extensive numerical study of a two-component binary mixture with interactions modeled by a very narrow SW potential. This mixture appears to be a logical extension of the one-component system for which crystallization is effectively avoided, by means of the geometrical rearrangements allowed by asymmetry in diameters of different particle species. The choice of a two-component system makes possible to extend the range of iso-diffusivity curves of almost 4 decades, as well as the range of studied packing fractions from approximately 0.57 for one-component to 0.62 for binary systems. One notes that at that highest density, the reentrance is so pronounced that an equivalent hard sphere system would be sufficiently dense to approach the 'random-close-packed' limit, though the definition of that concept has its own limitations [24].

The extension to a binary system does not only make more evident the reentrant behaviour of the glass transition curve, but also allows a deeper study of the dynamics of the system. By this we mean that it turns out to be possible to reach very closely the ideal glass line, intended as the $D \rightarrow 0$ locus of the (ϕ, T) -plane, and thus to feel quite clearly the presence of higher order MCT singularities. We know from the theoretical work that the 3%-case of the square well model possesses indeed an A_3 -singularity [4,5], corresponding to the end-point of the repulsive-attractive glass-glass transition. Though, of course, this singularity lies inside the glassy region, its presence is signaled by the characteristic logarithmic decay of density correlators mentioned above, already in the liquid region, when going sufficiently close to the neighbouring glass boundary.

We report in this paper a characteristic behaviour of the density correlators, near the ideal glass transition, which combines features of the typical A_2 singularity, i.e. simply ergodic to non-ergodic transition with two-step power-law relaxation, and of higher order singularities associated with logarithmic decay. This produces, in a certain region of the (ϕ, T) -plane, a new behaviour which cannot be described by the asymptotic predictions for either of the two behaviours, deriving by a competition of the two types of MCT solutions. The same kind of interesting result is found in the mean square displacement (MSD). This subtle interplay between different singularities is present also in theory, and its manifestation in simulation may be regarded as support for the theory, rather than an inconvenience. This will allow us to iden-

tify and localize quite clearly a genuine MCT higher order singularity in a realistic model.

II. SIMULATION AND THEORY

We study binary mixtures of SW spheres. In particular, we focus on samples of a 50% – 50% mixture of $N = 700$ spheres in a cubic box, with diameter ratio between the two species equal to 1.2. Thus, the smaller particles (B -type) diameter is $\sigma_B = 1$, and both A and B particles have unit mass. Both species interact with a square well potential with ratio between potential range and particle diameter equal to 3%. This corresponds to one of the cases studied theoretically within MCT, that clearly possesses all the main phenomena [4,5,25]. The 3%-ratio has been chosen also for interactions between particles of different species, i.e. we consider

$$\begin{aligned} V_{ij}(r) &= \infty & r_{ij} < \sigma_{ij} \\ V_{ij}(r) &= -u_0 & \sigma_{ij} < r_{ij} < \sigma_{ij} + \Delta_{ij} \\ V_{ij}(r) &= 0 & r_{ij} > \sigma_{ij} + \Delta_{ij} \end{aligned} \quad (1)$$

with $\epsilon_{ij} = \Delta_{ij}/(\sigma_{ij} + \Delta_{ij}) = 0.03$, $i, j = A, B$ and we use the conventional notation for which, for example, $\sigma_{AA} = \sigma_A$ and $\sigma_{AB} = (\sigma_A + \sigma_B)/2$. Temperature T is measured in units of energy, i.e. $k_B = 1$ and thus, for example, $T = 1$ corresponds to the system having a thermal energy equal to the well-depth, while the packing fraction is defined as $\phi = (\rho_A \sigma_A^3 + \rho_B \sigma_B^3) \cdot \pi/6$, where $\rho_i = N_i/L^3$, L being the box size and N_i the number of particles for each species.

Initial configurations for each density were chosen at random. Particles were separated in successive steps, with more particular care the higher the density of interest, to implement the hard core repulsion. When separation was ensured, the attractive well was added. To reach the temperature of study, the configuration so prepared was then left to evolve with a thermostat of constant thermal coefficient for a period of time sufficient to equilibrate at that temperature. We estimate the equilibration time as the time at which the density correlation function of the slowest collective mode (i.e. at the structure factor peak) has decayed to zero. After this equilibration, the configuration was left to run at constant energy for a time dependent on the slowness of the dynamics, for a time covering at least 10 equilibration times.

Simulation time for each species is measured in units of $\sigma_i \cdot (m/u_0)^{1/2}$. Standard MD algorithm has been implemented for particles interacting with SW potentials [26]. Between collisions, particles move along straight lines with constant velocities. When the distance between the particles becomes equal to the distance for which $V(r)$ has a discontinuity, the velocities of the interacting particles instantaneously change. The algorithm

calculates the shortest collision time in the system and propagate the trajectory from one collision to the next one. Calculations of the next collision time are optimized by dividing the system in small subsystems, so that collision time are computed only between particles in the neighboring subsystems.

We studied eight isothermal cuts of the phase diagrams, with temperature varying between 2.0 and 0.3 in the large packing fraction region, i.e. $\phi > 0.5$. In addition, we examined the hard spheres case, where no attractive interactions are present. For each considered configuration, we first studied the thermal history to check that, effectively, it maintains itself at the required temperature within fluctuations and that the total energy remains constant.

Of each studied configuration, we considered the time-dependent density correlation functions for different q -vectors to make direct comparison with the behaviour predicted by MCT. The correlators are defined as,

$$\phi_{ij}(q, t) = \frac{S_{ij}(q, t)}{S_{ij}(q)} = \frac{\langle \rho_i(-q, t) \rho_j(q, 0) \rangle}{\langle \rho_i(-q, 0) \rho_j(q, 0) \rangle} \quad (2)$$

where $\rho(\mathbf{q}, t) = \sum_l \exp(i\mathbf{q} \cdot \mathbf{r}_l(t))$ are the density variables for each species and $S_{ij}(q)$ are the partial static structure factors of the system. The $\phi_{ij}(q, t)$ are the fundamental quantities of interest in the Mode Coupling theory, which consists of writing a set of generalised Langevin equations, that can be closed within certain approximations [11,12,27,28].

The correlators $\phi_{ij}(q, t)$ have been calculated averaging over several independent configurations and over up to 100 different wave-vectors with the same modulus, to obtain a good statistical sample. Of course, these quantities show an interesting behaviour where the dynamics of the system gets slower, i.e. in the supercooled regime. Indeed, the relaxation process starts to show a separation in two time-scales, which originates the typical two-step relaxation scenario near the (ideal) glass transition. A first relaxation process, the so called β -relaxation, occurs at short times, due to particles exploring the cage formed by their neighbours, while a second process, the α -relaxation, that accounts for the restoration of the ergodicity due to breaking of the cages, occurs at larger and larger time scales, due to the slowing down of the dynamics, forming a longer and longer plateau region. At the ideal glass transition, the time of the α -relaxation diverges, and the correlators do not relax anymore, thus remaining at this plateau value. This is defined as the non-ergodicity parameter $f_{ij}(q) = \lim_{t \rightarrow \infty} \phi_{ij}(q, t)$, which jumps discontinuously from zero to a finite (critical) value $f_{ij}^c(q)$, signaling the occurrence of an ergodic (fluid) to non-ergodic (glass) transition.

The two-step relaxation is well described by MCT, through an asymptotic study of the correlators near the ideal glass solutions. The approach to the plateau is described by a power law, regulated by the exponent a , i.e.

$$\phi_q(t) - f_q^c \sim h_q^{(1)}(t/t_0)^{-a} + h_q^{(2)}(t/t_0)^{-2a} \quad (3)$$

with t_0 the microscopic time, while the departure from the plateau, i.e. the start of the α -process, is expressed in terms of another power law, regulated by the exponent b ,

$$\phi_q(t) - f_q^c \sim h_q^{(1)}(t/\tau)^b + h_q^{(2)}(t/\tau)^{2b} \quad (4)$$

with τ the characteristic time of the relaxation. The exponents a and b are related to each other with an algebraic relation, and are independent of the particular q -vector considered, $h_q^{(1)}$ and $h_q^{(2)}$ are called critical amplitudes [12].

On the other hand, the α -relaxation process can be also well described by a stretched exponential, i.e.

$$\phi_q(t) = A_q \exp[-(t/\tau_q)^{\beta_q}] \quad (5)$$

where the amplitude A_q determines the plateau value, and the exponent β_q is always less than 1.

We can thus fit the correlators, for each q -value considered, both in terms of the MCT prediction and of the stretched exponential, and find an estimate of the non-ergodicity factor f_q as a function of q . The shape of this quantity can be indicative of the formation of different types of glasses, either attractive or repulsive dominated [1,2,4,5].

However, what we have described so far is typical for A_2 singularities. These correspond to the simplest non-trivial solutions for the non-ergodicity parameter MCT equations, and for example in the hard sphere model only this type of singularity can arise. This is due to the fact that the only control parameter of the model is the packing fraction. When the number of control parameters increases, higher order singularities may occur. For a square well model it was shown that singularities of types A_3 and A_4 are present within the theory [4] when the width of the well becomes much smaller than the hard core radius. In the proximity of such singularities, the asymptotic behaviour for the density correlators is different from the one we have seen so far [4,13]. In particular, we have for the leading contribution a logarithmic behaviour,

$$\phi_q(t) - f_q^c \sim -C_q \ln(t/\tau) \quad (6)$$

Another main focus of our study was to evaluate the MSD $\langle r^2(t) \rangle$ of particles with respect to their initial positions. We considered a configuration to have sufficiently evolved when particles on average have traveled further than a few diameters.

Typically, the behaviour of the MSD at short times, follows the simple law $\langle r^2(t) \rangle \sim t^2$, which accounts for the ballistic motion of the particles, i.e. particles move freely without collisions. At later times, particles start to

feel the presence of each other and there is crossover to the diffusive regime, i.e. $\langle r^2(t) \rangle \sim t$. The proportionality constant of this relation defines the diffusivity of the system, via the celebrated Einstein relation [29],

$$\lim_{t \rightarrow \infty} \frac{\langle r^2(t) \rangle}{t} \simeq 6D \quad (7)$$

Thus, from evaluating the long time limit of the MSD, we determine the diffusion coefficient D for each state point.

Though this general behaviour is preserved, when the dynamics becomes slower, a transient region between short and late times emerges. Of course, the duration of this transient region increases the slower the dynamics. This phenomenon is the correspondent behaviour for the MSD of the separation of the two time scales that we have seen in the correlation functions. It also reflects the formation of cages in which particles get trapped, so that diffusion becomes more difficult. The crossover region consists generally in the development of a plateau also for the MSD. At the ideal glass transition, the α -relaxation time would diverge, and diffusion from the plateau would not occur even at infinite times, in complete analogy with the correlators behaviour. Thus, the height of the plateau represents the localization length of particles in the arrested state, i.e. the size of the cages of the glass. Of course, in simulations, only finite times can be explored and the position of the ideal glass transition can be only extrapolated by data.

As for the correlators, the presence of higher order singularities may affect the plateau region of MSD, giving rise to peculiar new behaviour.

MCT predicts a power law decrease for the diffusivity on approaching the ideal glass transition. Along an isotherm

$$D \sim |\phi - \phi_c|^\gamma \quad (8)$$

where ϕ_c is the value of the packing fraction at the transition ('critical' value), i.e. the value where the diffusivity would drop to zero for the considered temperature. The exponent γ is completely determined by the theory in terms of the exponents a and b , via the simple relation $\gamma = 1/(2a) + 1/(2b)$ [12]. It is also related to the so-called exponent parameter λ by an analytical relation. This parameter is crucial in determining the presence of higher order singularities [4], in particular it tends to the value $\lambda = 1$ at an A_3 -point, while for a simple A_2 singularity is always less than 1.

So, in principle, from fitting the diffusivity behaviour at constant temperature with Eq. 8, one can determine the exponent γ , and from this, also a and b . From a fitting procedure based on Eq. 4, the non-ergodicity parameter can be calculated consistently. However, close to higher order singularities, we do not expect that this behaviour is generally preserved, as the logarithmic behaviour in the correlators and the transient region in the

MSD intervene. Indeed, in these conditions, the exponent b tends to zero (thus originating the logarithmic behaviour) and, from the relation between b and γ , one can see that γ would go to ∞ , and Eq. 8 cannot then describe the arrest. Thus, the region of validity of asymptotic predictions may shrink significantly close to higher order singularities.

III. RESULTS: THE OVERALL PICTURE

The considered mixture represents a natural extension of the mono-disperse system studied so far [17]. Indeed, the small asymmetry in diameter does not produce significant change in the dynamics of the two cases, and, on the contrary, allows to reach much larger packing fractions with no sign of crystalline order. The first of the two sentences can be explained by looking at Figure 1. Here, we compare the behaviour of density correlators at a correspondent point on the control parameter space of the system. For the mono-disperse case we are almost at the most reentrant point before crystallization takes place, i.e. $\phi = 0.57$ and $T = 0.75$. We can clearly see that, nonetheless, dynamics does not appear to be particularly slowed down. To make the comparison with the binary case, we are considering the total density correlation function for the species 1 at the q -vector corresponding approximately to the first peak of the static structure factor, and quantities have been rescaled in order to compare particles with equal diameters. It is evident that the dynamical behaviours are very close, thus in this sense, we can think of doing an extension of the one-component work.

In the following, we will focus on properties of particles of type A . Thus all quantities reported without label, will refer to them. This choice derives from the fact that we do not expect substantial differences in the behaviour of the two species, due to the small amount of asymmetry in their sizes.

We start by comparing the T and ϕ dependence of the diffusion coefficient. The diffusion coefficients can be normalised with respect to the factor $D_0^i = \sigma_i \sqrt{T/m}$, which takes into account the T -dependence of the microscopic time. This ensures that the difference in the average velocities due to the temperature is eliminated, and the diffusion can be considered to be comparable between different temperatures.

A plot of the D_A/D_0^A in function of packing fraction, along the considered isotherms, is shown in Fig. 2. In the present work, we focus our attention mainly on the high densities regime, i.e. $\phi > 0.5$. The behaviour of the diffusivities presents many similarities with the case of a mono-disperse sample of SW spheres [17]. However, striking novel features appear due to the fact that, for the chosen binary system, it is possible to reach diffusivities

4 orders of magnitude smaller than in the mono-disperse case, as well as much larger packing fractions with no sign of crystallization.

We present results of normalised diffusivities varying roughly between 10^{-2} and 10^{-6} , while the mono-disperse system could only reach values up to slightly above 10^{-2} , due to the intervening of crystallization [17]. We remark that the lowest diffusivity values were imposed by computational times, and not as in the mono-disperse by crystallization. Also, the attractive binary system is able to occupy effectively a larger amount of available volume, thus reaching liquid states up to a packing of about 0.62. On the other hand, the hard spheres case reaches comparable values of diffusivities at a packing fraction of about $\phi = 0.585$ (see Fig. 4), a value close to the one experimentally established for the one-component hard sphere case [30].

Examining the figure, it is evident that the behaviour of the diffusivity is driven by two competing mechanisms. Upon decreasing temperature starting from the highest value, the presence of the repulsive core, initially dominant, enters in competition with the attractive interactions. This is manifested in the diffusion getting larger, at the correspondent packing fraction, by decreasing temperature. In other words, the system reaches the same diffusivity at larger and larger packing fractions. This is due mainly to geometrical rearrangement of particles, as the temperature is lowered, i.e. particles tend to get closer and, consequently, more free space for diffusion gets available to the system. However, when the temperature becomes small enough, i.e. effectively lower than the energy scale of the square well, attractions become dominant and thus, diffusion becomes slower again because particles tend to remain within each other shell of attraction.

We know from theoretical calculations within MCT that this phenomenon is typical of very narrow attractive potentials, both for square well interactions [4] and for hard-core Yukawa [6]. Indeed, the 3%-choice for the range of the attractive well in our simulation corresponds to ensure that competition between attraction and repulsion is particularly sharp. This can be explained in terms of cages, i.e. when the attractive range is not small enough, which means few percents of diameter, there is not much difference between cages formed by neighbouring particles at high or low temperatures. On the other hand, a very localised attraction can effectively change the shape of the cages, by sticking particles within the well-distance Δ . This produces the larger diffusions observed at intermediate temperatures, when the two mechanisms almost balance each other. Similarly, extremely short-ranged attractions produce a solid-solid iso-structural transition, between an attractive-dominated and a repulsive-dominated crystal [31]. This has been correlated with the glass-glass transition predicted by MCT in a recent work [6]. Of course,

it would be interesting to extend the simulations to different values of the range of the potential to confirm the width dependence of the anomalous behaviour.

Observing more carefully Figure 2, the two mechanisms of diffusion produce two different trends of behaviour for the plotted curves. Indeed, for $T > 0.6$ the curves present a quite dramatic decrease of diffusivity, while for smaller temperatures the same decrease of about 4 orders of magnitude occurs on a much wider range of packing fractions (for example comparing $T = 2.0$ and $T = 0.4$ such range almost doubles).

We also note that, if we plot the bare diffusion coefficients, as evaluated from the fit of the MSD, without normalising by D^0 , the reentrant behaviour is preserved. This can be an advantage, from an experimental point of view, because it would allow to observe at the same packing fraction for various temperatures the diffusivity firstly increasing then decreasing again, without having to include the thermal factor. We plot in Fig. 3 the not-normalised diffusivities at fixed packing fractions, varying the temperature. The appearance of a maximum, sharper with increasing density, is indeed another manifestation of the reentrance. Extracting the values of maximum diffusivity, it is possible to draw a ‘maximum diffusion’ line in the phase diagram. This could be interesting as, for example, in a complex system like water, this line appears to play a very important role in the understanding of the ‘metastable’ part of the water phase diagram [32].

To make contact with the theoretical results for the ideal glass transition, we have extrapolated curves of normalised iso-diffusivities, as for the mono-disperse case [17] and represented them in Figure 4. Of course, the limit $D \rightarrow 0$ would correspond to the ideal glass line, as calculated by MCT. We report the curves for normalised values varying between $5 \cdot 10^{-3}$ and $5 \cdot 10^{-6}$, and in the inset we present for comparison the ideal glass line as predicted by MCT for a SW one-component system.

It is interesting to comment on the behaviour of the iso-diffusivity curves. Depending on which diffusivity value is chosen, the most reentrant point, i.e. the (ϕ, T) -point characterized by largest packing fraction with that diffusivity, changes. In the considered range of diffusivities, its temperature varies from 0.75, which also corresponds to the most reentrant point for the mono-disperse case, to 0.5. However, data of Fig. 2 allow to say that, in the limit $D \rightarrow 0$, such point will be found at a finite temperature between 0.4 and 0.5, since the reached packing fractions are so large that it would not be possible, within the trend, to go much beyond.

The reentrant behaviour, present in Mode Coupling calculations, is then confirmed by simulation. It is clear that, since MCT underestimates the effect of packing, we should not expect, a perfect quantitative agreement between theory and numerical results. Indeed, for example for the simple hard sphere case, the MCT critical glass

transition packing fraction is $\phi \simeq 0.516$ [33] whereas in experiments this has been shown to be $\phi \simeq 0.58$ [30]. On the other hand, the same experiments have shown that more accurate predictions can be expected for the behaviour of dynamical quantities such as the density-density correlation functions and the MSD.

IV. RESULTS: DYNAMICS ALONG ISOTHERMS

We start by examining the results for the isotherm $T = 2.0$. Here particles have sufficient thermal energy to escape the attractions and the resulting dynamics appears to be quite similar to that expected for ordinary hard spheres. However, the effect of the attraction, thought not changing the general behaviour, is to enlarge the liquid part of the phase diagram toward packing fractions already quite larger than the typical (one-component) hard sphere value, i.e. 0.58. At this temperature, indeed, the system behaves as a fluid at least up to a packing fraction $\phi = 0.595$, where the time limit of our simulation is reached. Close to this limit value, the diffusivity decreases almost two orders of magnitude for a variation of 1% in packing fraction.

In Figure 5(a) we report the time-dependent density-density correlators at increasing packing fraction, up to the closest to the ideal glass transition. The dramatic decrease in diffusivity is reflected in the behaviour of the correlators by the formation of the typical two step relaxation process near the arrest, described above. Similar behaviour can be also observed in the behaviour of the MSD displayed in Fig. 5(b) in unity of σ^2 . We note, however, that the height of the plateau of approximately 10% of particles diameter is consistent with Lindemann's melting criterion [34].

The diffusivity data can be fitted with the MCT power-law behaviour (Eq. 8). This holds sufficiently close to the ideal glass transition, thus we considered relevant for the fit only those points for which a clear α -relaxation process was evident. Doing so, we found $\gamma \simeq 3.6 \pm 0.4$. This value is already much larger than the typical one-component hard sphere value predicted by MCT, i.e. $\gamma^{HS} = 2.58$ [33]. In the case of our particular binary mixture, in the hard sphere case, whose diffusivity behaviour is also reported in Fig. 2, we found a value of $\gamma = 2.9 \pm 0.2$. The uncertainty on the exponent is due to the variation it gets when considering only the points closest to the transition. We note that in reference [8], the case reported brings a value of $\gamma = 3.03$. Thus, we are in a situation clearly closer to a higher order singularity, being the correspondent other MCT exponents for this value, respectively $b = 0.35$ and $\lambda = 0.874 \pm 0.03$. It is perhaps important to stress at this point that the value of γ obtained with this procedure can be slightly wrong due to the difficulty to get close enough to the ideal glass transition with numerical simulations [35]. We will use the

so-calculated value of b in the next paragraph to fit the behaviour of density correlators along the iso-diffusivity curve $D/D_0 = 5 \cdot 10^{-6}$, to give an idea of the behaviour of quantities of interest along the ideal glass transition line.

The case $T = 1.5$ shows a behaviour completely analogous to $T = 2.0$. We note however that the fit of the diffusivity with Eq. 8 gives in this case the exponents $\gamma = 3.8 \pm 0.5$, $b = 0.325$ and $\lambda = 0.888$. The increase in the value of λ is expected since we are getting closer to the reentrant region, and consequently to the singularity. The same trend is observed for $T = 1.0$ with γ still increasing up to about 3.96 ± 0.12 , and λ reaching the value of 0.896.

At $T = 0.75$ a new interesting behaviour appears. Indeed, in the density correlators a logarithmic decay starts to emerge. As shown in Fig. 6, some state points display a logarithmic decay (see curve for $\phi = 0.58$ in the figure) for almost the whole relaxation process, i.e. after the microscopic relaxation up to complete decay. The shape of this logarithmic behaviour appears quite different from the one found in reference [8]. On the other hand, it reminds quite closely the shape of MCT correlators near the A_3 singularity for the 3% square well potential reported in Figure 11 of Ref. [4], which for comparison is reported in the inset in Fig. 6. Upon increasing density, and so getting closer to the glass transition, the relaxation changes to the usual two-step form, clearly indicating a similar situation of our isothermal path to that indicated in the inset of Fig. 11 cited above. Thus, the higher order singularity dominates the dynamics at smaller packing fractions, but when one gets sufficiently close to the glass transition, a conventional A_2 singularity is met, and this causes the restoration of the typical α -relaxation. By considering only those packing fractions, when at least the beginning of the α -relaxation can be observed (i.e. $\phi > 0.6$), we can fit the diffusivity again with Eq. 4, obtaining the extremely high value $\gamma \sim 5.1$, corresponding to the value of $b \sim 0.25$ and $\lambda = 0.937$. We cannot here estimate the error, due to the small number of points available (only five for three parameters for the fit), however, even if not so precise, it clearly indicates we are approaching a higher order singularity. As we shall see by looking at the shape of the non-ergodicity factors in the next paragraph, we can anticipate that we are meeting the A_2 line along its repulsive branch, again as in the inset of Fig. 11 of ref. [4], but probably at a slightly higher temperature.

The last observation derives from the analysis of the $T = 0.6$ isotherm. The correlators, reported in Figure 7(a), show an even closer behaviour to the one predicted by MCT in [4] (again Fig.11, i.e. inset of Fig. 6). However, at this temperature, the two competing singularities must be so close to each other that a clear α -relaxation does not take place within the reach of our simulation, i.e. the logarithmic behaviour remains always

very important, and even at higher packing fractions it is clearly observable before the α -process takes over. The interesting feature emerging is that, in all the cases considered the logarithmic behaviour does never extend for much more than 3 and a half decades in time. This arises because, in the present topology of the phase diagram, one is either close to the A_2 -singularities to observe a pure logarithm, or is too far from the glass transition and thus the relaxation time is generally not too large. Indeed, this behaviour is strongly supported again by the theoretical calculations in [4].

It is to note that at this temperature we are not able to convincingly fit the power-law density dependence of the diffusivity. Indeed, if one forces the fit on the points, one find exponents strongly dependent on the selected ϕ range. A possible explanation for this data sensitivity to ϕ can be found in the competition between type A_2 and A_3 or A_4 dynamics. In such condition, only a comparison with a full MCT solution (as opposed to an asymptotic prediction) may help in rationalizing the density dependence of diffusivity. In agreement with the previous observations, also the MSD, represented in Figure 7(b) starts to show deviations from usual type B behavior. Indeed, a clear flat region does not appear, though dynamics are significantly slow. What can be observed is a slight deviation from the flat region found at higher temperatures, which will become more and more evident at lower temperatures. No clear localization length can be found. Attraction at this temperature has become quite relevant. It is again a sign of very strong competition between different singularities, between attractive and repulsive cages.

Upon further decreasing temperature, we enter the most delicate region of the phase diagram. Indeed at $T = 0.5$, as for $T = 0.6$, it is not possible to find any MCT exponents, and the situation gets even worse in interpreting the behaviour of the correlators. These are plotted in Figure 8(a). Indeed, no clear behaviour, at all densities, either logarithmic or of type α , can be individuated, and no evident plateau value ever arises. We note that the long-time decay of density correlators can be represented by a stretched exponential, but with very low exponents β_q , as shown in Figure 9. In the MSD, reported in Figure 8(b), the phenomenon present at the previous temperature, becomes more accentuated. Even the slowest studied state point is far from being asymptotic, and the MSD presents a clear transient region.

The case where the anomalous dynamics and the interplay between different singularities is fully displayed is offered by the $T = 0.4$ isotherm. The correlation functions, shown in Figure 10(a), are rather peculiar. Even the long time limit is far from being rationalized in term of stretched exponential decay. The MSD behaviour, shown in Figure 10(b) is also quite intriguing. The MSD transient behaviour is now evidently of a peculiar type. Indeed, for about 4 decades in time, it shows

a dependence which can be quite accurately described by a power-law behaviour, i.e.

$$\langle r^2 \rangle \sim t^x \quad (9)$$

We estimated via a fit $x \simeq 0.44$. A similar behaviour has been found in the MCT study of polymeric systems [36], for displacements varying from the typical localization length of hard-sphere-like cages to end-to-end distance. The analogy with the polymeric systems, where permanent bonds are present (in a sense close to the attractive cages at this very low temperature), can be a guide to a deeper understanding of this regime.

The strong effects that we find at this value of temperature seem to suggest that along this isotherm the system approaches the closest point to the singularity, even if we do not know yet on which side (attractive or repulsive) of the glass line it will be located. To understand the nature of the dynamics which takes place here further investigations are needed, and maybe a more complete analysis of the correlators, and a comparison with full solutions of the MCT equations.

Finally we analyze the last isotherm, corresponding at $T = 0.3$. This being a very low value for the system to equilibrate, data are not so clean as for the other cases, also because here one needs to study slower points with respect to the other temperatures in terms of bare diffusivities, to reach the same values of normalised ones. However, despite these technical difficulties, we find more transparent results in terms of conventional MCT interpretations, i.e. we can identify the development of a two-step process typical of an A_2 singularity, both for the correlators and for the MSD than in the previous case.

Indeed, observing the correlators in Figure 11(a), it is clear that, close enough to the transition, they present the development of a plateau, and thus, an α -relaxation process, as shown in the inset of the figure for various q -vectors. However, this plateau is extremely high, and clearly indicates that we are now undoubtedly in the condition of attractive glasses. It is of deep interest to note the analogy of this behaviour with the one that has been found in the study of ‘strong’ gels [37], even if this should be inspected at lower densities also. Despite this clear behaviour, even at this temperature, it is not possible to evaluate unambiguous power-law exponents from the diffusivity. Figure 11(b), represents the evolution of MSD at this temperature. Here, a signature of a localization length, smaller than the one in the high temperature cases, starts to develop. Indeed, an indication of a plateau is observable around $\langle r^2 \rangle = 0.0006 \cdot \sigma^2$. The corresponding localization length is of the order of Δ , supporting the interpretation that at this temperature the relevant localization length has become the attractive well. In this respect, one can interpret the sub-diffusive behavior of the MSD discussed at $T = 0.4$ as a cross-over effect between the hard-sphere and attractive well differ-

ent localization lengths, in a similar fashion to what has been obtained for polymeric systems [36].

V. RESULTS: ALONG THE ISO- D/D_0 CURVE

We now focus on studying the behaviour of correlators and MSD, and other quantities along the iso-(normalised)-diffusivity, i.e. iso- D/D_0 , curve $D/D_0 = 5 \cdot 10^{-6}$, shown in Fig. 4, which represents our closest available representation of the ideal glass transition line. The aim of this study is to give clear evidence of the existence of two distinct glassy states, attractive and repulsive. Also, it aims to connect even more closely this simulation to the MCT calculations, which also were performed in a similar fashion, along the ideal glass lines, in ref. [5].

We start by representing the behaviour of density correlators along the iso- D/D_0 line in Figure 12. The curves here represented, having equal diffusivity, also have the same normalized relaxation time. Thus, we can clearly see the change in the decay which takes place, upon decreasing temperature, from a marked α -relaxation at higher temperature to the extremely slow decay of $T = 0.4$, passing through the intermediate regimes between $T = 0.75$ and $T = 0.5$. Of course, here, no evident logarithmic behaviour can be observed, due to the proximity to the A_2 transition, as discussed in the previous paragraph.

Next, we report the MSD behaviour along the line in Figure 13. Despite the larger statistical error at $T = 0.3$, we display them as an important part of the whole picture. Thus, here, we can clearly observe the change in the diffusion process. The first evident thing to note is the big gap, of almost 2 orders of magnitude, in the localization length of particles, which, as discussed above, characterises the size of cages around particles. Clearly this fact can be used as a justification to speak of ‘attractive’ cages, opposed to normal cages, intended as simple occupation of the available space. In the attractive cages, the average distance between particles is much smaller, the lower the temperature. This is the first clear signal of different structure in the glass formation.

Also, we can also examine more carefully the modification of the plateau present at higher temperatures, in the transient regime. Indeed, increasing the attraction, this tends to bend downwards until a sort of ‘saturation’ between the two competing mechanisms (attraction and packing) take place, corresponding to the sub-diffusive behaviour of $T = 0.4$. After this point, attractions become dominant, and the curve starts to bend upwards. This might suggest that, going at even lower diffusivities, the MSD would display a similar plateau as for high temperatures at roughly $\langle r^2 \rangle \sim 0.0007 \cdot \sigma^2$ [38], which means roughly a localization length of 2.6% of the particle diameter, i.e. comparable with the width of the

attractive well of the model, confirming our conjectures on the formation of attractive cages, or, to use another expression, bonds. However, to gain further evidence on how these mechanisms really happen and evolve in the system, a specific study of configurations in terms of average distance, sizes of clusters, and heterogeneities in general should be performed, and this is beyond the aim of the present work. We note that a similar figure, showing the behaviour of MSD with attraction, has appeared in [9], but not all of these considerations could be made there, due to the distance from the transition.

We now turn to evaluate the non-ergodicity factor f_q along the iso- D/D_0 curve. To do this, we have fitted the density correlators at various q -vectors, and extracted the relevant parameters. Where possible, i.e. where the power-law behaviour for the diffusivity in (8) was found to be valid, we used the power-law described in terms of the b exponent for the α -relaxation of equation (4). Thus, for $T = 2.0$, we implemented the fit with $b = 0.35$, while respectively for $T = 1.5, 1.0, 0.75$ we used $b = 0.32, 0.31, 0.25$. These values have been found very good for the fits, always finding a χ^2 of the order of 10^{-4} or less. For lower temperatures, it was not possible to use this strategy and, consequently, we had to use the approach of the stretched exponential in Eq 5, and use its amplitude as an estimate for f_q . The parameters of the fits, i.e. the exponent of the stretching β_q and the relaxation time τ_q , for the considered temperatures $T = 0.6, 0.5, 0.3$ are reported in Fig. 9 to display their q -behaviour. Even though the stretched exponential law is not analytically justified, it is quite established in the literature to use it as a fitting law for extracting the non-ergodicity parameter [35]. In the case of $T = 0.4$ also this strategy did not work, as already discussed [39].

In Figure 14 we show the so-calculated f_q . Amazingly, from $T = 2.0$ down to $T = 0.6$, they all collapse onto the same curves, giving a strong evidence of MCT predictions for the repulsive glass [5]. Thus, the repulsive glass is independent of temperature, and also this shows how the passage to attractive glass intervenes quite sharply. For lower temperatures, the glass becomes then attractive, and the non-ergodicity parameter starts to be modified with temperature, becoming finite also at much larger q -vectors [5]. Despite some errors generated by the stretched exponential fits at these low temperatures or the data noise at $T = 0.3$ a significant change in the shape and width of f_q is seen between $T = 0.5$ and $T = 0.3$. It could be that the case at $T = 0.5$ is quite sensitive to the singularity, and thus it is a somehow intermediate case. A more detailed study, either theoretically or by considering intermediate or even lower temperatures for smaller packing fractions, will be helpful for clarifying this issue. On the other hand, the establishment of the existence of the two glasses along the line appears to be definite by these results. To support this statement, we

have plotted in Fig. 15 both the (partial) static structure factor $S_{AA}(q)$ (rescaled by a factor of 2 for having a better visualization of the figure) and the non-ergodicity factor, respectively at the highest, $T = 2.0$, and at the lowest, $T = 0.3$, temperatures studied in this work, so to compare the most extreme cases of repulsive and attractive glasses. Firstly, we note how the oscillations of the non-ergodicity factors follow the ones in the structure factor quite closely in both cases (for the $T = 0.3$ case, the scale of the figure almost flattens these oscillations, which are more evident in Fig. 14). Also, the $S(q)$ presents the typical features we expected from theoretical calculations within MCT and integral equations. Indeed, the repulsive case shows a marked first peak, which is the main responsible for the glass transition, while the attractive one possesses larger secondary oscillations, that constitute a signal of the smaller cages already described above. Thus, this contributes to establish not only the existence of the two glasses, but also, and most importantly, the two distinct mechanisms which drive the glassification in the two cases, i.e. simply packing and localised attraction.

VI. CONCLUSIONS

In this paper, using molecular dynamics, we have studied the dynamical arrest phenomena of spherical particles interacting via a square well potential. The square well potential has been studied as one of the simplest canonical models of solids liquids and gases for many years [18–23]. Here we have extended the models applicability to the domain of dynamical arrest, and glassy phenomena. Previous predictions for dynamical arrest from mode coupling theory for the square well potential are available [4,5], so direct comparisons are feasible.

By using a well-adjusted binary mixture, we have been able to extend our previous preliminary investigations [17] much closer to the arrest transition, accessing diffusion constants that are 4 orders of magnitudes smaller than in the previous calculations. Nevertheless, results on the lowest valued iso-diffusivity curve available for the single-component system are very close to those for the binary mixture, so we may consider the role of the second component to be mainly the prevention of crystallization.

In that regime where repulsions dominate, we recover an ideal-glass-transition with power law scaling of the diffusion constant. We also find an attractive branch to the dynamical arrest where theory has predicted the presence of an 'attractive' glass. Where attractions and repulsions compete in nearly equal terms we find re-entrance in the arrest curves when plotted in units of the microscopic temperature dependence of the diffusion constant. However, fixed-density diffusion constants, plotted without any normalization, exhibit a maximum in the diffusion constant as temperature is increased. This maximum

locates the re-entrant liquid where mobility is anomalously high. We consider that the essential features of re-entrance in this regime for the square-well potential now to be confirmed, in agreement with the predictions of theory [4].

We have studied also the evolution of the density-density correlation functions (dynamical structure factors) and, independently, the mean-squared distance traveled by particles in the vicinity of the reentrant regime. As expected, where repulsive interactions dominate, we find the classical arrest scenario in which plateaus develop in both functions as arrest is approached [14]. These plateaus indicate the development of an observable characteristic cage time, and are quite typical of prediction by MCT for hard sphere systems. When attraction begin to compete on equal terms, in the vicinity of the re-entrant regime, the theory has predicted the existence of an A_3 singularity embedded in the arrested region. It is therefore difficult to access this singularity directly by molecular dynamics, but the theory has indicated that there are distinctive signatures of this singularity in the re-entrant fluid phase, on approach to arrest. In particular, density correlators from a suitable fixed-temperature cut of the phase diagram have an interesting pattern of behavior in which the logarithmic behaviour [13], due to the embedded A_3 point, first begins to dominate, and then crosses over to the conventional A_2 singular behavior more commonly observed for normal MCT arrest. The density correlators in the re-entrant regime clearly exhibit this phenomenon, the pattern of evolutions being essentially in agreement with the predictions of theory.

We may pause here to comment that we do not regard this complex cross-over behavior as a complication, but in fact as a rather delicate, and unusual signature of the whole re-entrant phenomenon, and interplay between A_2 and A_3 singularities. That the simulations would reproduce this is strong support for the detailed picture offered by theory. The behaviour of the mean-squared displacements are also quite unusual, and there is as yet no theoretical prediction for them in this regime.

Finally, we are able to extract the non-ergodicity factors along the arrest curve, for the lowest iso-(normalised)-diffusivity constant curve. Again, in line with theoretical predictions we find strong evidence of a transition from a repulsive glass to attractive glass behavior, as indicated by the change in characteristic shapes of the non-ergodicity factors. This is the first direct evidence of the repulsive glass-to-attractive glass transition that has been predicted by the theory, representing one of the most remarkable phenomena associated with the system.

The theory suffers from strong systematic shifts of all the arrest curves in relation to the simulated ones, a phenomenon long known from the example of the hard sphere. However, in detail the theoretical predictions

of re-entrant regime, with associated crossover to logarithmic singularity, and glass-to-glass transition has been confirmed by detailed molecular dynamics calculations.

From the experimental point of view, there is accumulating evidence that all the phenomena described here are robust, being relatively independent of the details of the experimental system used to study them [15,16,9]. The same is true of the theoretical studies [1,2,4-7] and simulations [8,17]. The square well potential is one of the simplest examples one can study, and it is reassuring that it exhibits the phenomena.

Our original prediction that in the dense regime, colloidal particulates system with short-ranged potentials could be described using ideas from dynamical arrest and glass theory now seems to be strongly supported. Dense particle gels are thereby identified as an example of a new type of glass, or dynamically arrested phase. The implications are broader than the simple example studied, for it indicates that it may be possible to interpret many formerly disparate phenomena such as coagulation, precipitation, aggregation, and gellation within the paradigm of dynamical arrest or glass theory. This is a fundamental soft of perception in the field of dense soft-condensed matter which may prove to be very fruitful in coming years.

This research is supported by the INFM-HOP-1999, MURST-PRIN-2000 and COST P1. S.B. thanks the University of Rome and NSF, Chemistry Division (Grant No. CHE0096892) for support.

-
- [1] J. Bergenholtz and M. Fuchs, Phys. Rev. E **59**, 5706 (1999).
- [2] L. Fabbian, W. Götze, F. Sciortino, P. Tartaglia and F. Thiery, Phys. Rev. E **59**, R1347 (1999).
- [3] G. Foffi, E.Zaccarelli, F. Sciortino, P.Tartaglia and K.A. Dawson J.Stat.Phys, **100**, 363 (2000).
- [4] K. A. Dawson, G. Foffi, M. Fuchs, W. Götze, F. Sciortino, M. Sperl, P. Tartaglia, Th. Voigtmann and E. Zaccarelli, Phys. Rev. E **63**, 1140 (2000).
- [5] E.Zaccarelli, G.Foffi, P.Tartaglia, F.Sciortino and K.A.Dawson Phys. Rev E, **63**, 031501 (2001).
- [6] G. Foffi, G. D. McCullagh, A. Lawlor, E. Zaccarelli, K. A. Dawson, F. Sciortino, P. Tartaglia, D. Pini and G. Stell, Phys. Rev. E **65**, 031407 (2002).
- [7] K. A. Dawson, G. Foffi, G. D. McCullagh, F. Sciortino, P. Tartaglia and E. Zaccarelli, J. Phys.:Condens. Matt. **14**, 2223 (2002).
- [8] A. M. Puertas, M. Fuchs and M. E. Cates, Phys. Rev. Lett. **88**, 098301 (2002).
- [9] K.N. Pham, A. M. Puertas, J. Bergenholtz, S.U.Egelhaaf, A. Moussaid, P.N. Pusey, A.B. Schofield, M. E. Cates, M. Fuchs and W.C.K. Poon, Science **296**, 104 (2002).
- [10] K. A. Dawson, Curr. Opin. Colloid Int. Sci., in press (2002).
- [11] U. Bengtzelius, W. Götze and A. Sjölander, J. Phys. C **17**, 5915 (1984).
- [12] W. Götze in *Liquids, Freezing and Glass Transition* edited by J.P. Hansen, D. Levesque D, and J. Zinn-Justin (Amsterdam: North-Holland) p 287, 1991.
- [13] W. Götze and M. Sperl, Phys. Rev. E (in press), 2002.
- [14] W. Götze, J. Phys.: Condens. Matter **11**, A1 (1999).
- [15] E. Bartsch, M. Antonietti, W. Shupp and H. Sillescu, J. Chem. Phys. **97**, 3950 (1992); E. Bartsch, V. Frenz, J. Baschnagel, W. Schärfl and H. Sillescu J. Chem. Phys. **106**, 3743 (1997); A. Kasper, E. Bartsch and H. Sillescu, Langmuir **14**, 5004 (1998).
- [16] F. Mallamace, P. Gambadauro, N. Micali, P. Tartaglia, C. Liao and S. H. Chen, Phys. Rev. Lett. **84**, 5431 (2000).
- [17] G. Foffi, K. A. Dawson, S.V. Buldyrev, F. Sciortino, E.Zaccarelli and P. Tartaglia, Phys. Rev. E **65**, 050802 (2002).
- [18] B.J.Alder, D.A. Young and M.A. Mark J.Chem.Phys.**56**, 3013 (1972).
- [19] M.G. Noro and D. Frenkel, J.Chem.Phys. **113**, 2941 (2000).
- [20] J.R. Elliot and L.Hu J.Chem.Phys. **110**, 3043 (1999).
- [21] L. Vega, E. de Miguel, L.F. Rull, G. JACKSON, and I.A. McLure J.Chem.Phys. **96**, 2296 (1996).
- [22] J. Chang and S. I. Sandler Mol. Phys. **81**, 745 (1994).
- [23] C. Rascon, L. Mederos and G. Navascues, Phys. Rev. Lett. **77**, 2249 (1996).
- [24] S. Torquato, T. M. Truskett and P. G. Debenedetti, Phys. Rev. Lett. **84**, 2064 (2000).
- [25] K. A. Dawson, G. Foffi, F. Sciortino, P. Tartaglia and E. Zaccarelli, J. Phys.: Condens. Matt., **13**, 9113 (2001).
- [26] D. C. Rapaport, *The Art of Molecular Dynamic Simulation*, Cambridge University Press, 1995.
- [27] E. Zaccarelli, G. Foffi, F. Sciortino, P. Tartaglia and K. A. Dawson, Europhys. Lett. **55**, 139 (2001).
- [28] E. Zaccarelli, P. De Gregorio, G. Foffi, F. Sciortino, P. Tartaglia and K. A. Dawson, J. Phys.: Condens. Matt. **14**, (2002).
- [29] J.P. Hansen and I.R. McDonald, *Theory of Simple Liquids*, London: Academic Press (1986).
- [30] W. van Megen and S. M. Underwood, Phys. Rev. Lett. **70**, 2766 (1993), Phys. Rev. E **49**, 4206 (1994).
- [31] P. Bolhuis and D. Frenkel, Phys. Rev. Lett. **72**, 2211 (1994); P. Bolhuis, M. Hagen and D. Frenkel Phys. Rev. E **50**, 4880 (1994).
- [32] A. Scala, F.W. Starr, E. La Nave, F. Sciortino, H.E. Stanley *Nature* **406**, 166 (2000).
- [33] J. L. Barrat, W. Götze and A. Latz, J. Phys. Condensed Matter **1**, 7163 (1989).
- [34] N. W. Ashcroft and N. D. Mermin, *Solid state physics*, Fort Worth-London, (1976).
- [35] M. Nauroth and W. Kob, Phys. Rev. E **55**, 657 (1997); A. Rinaldi, F. Sciortino and P. Tartaglia, Phys. Rev. E **63**, 061210 (2001).
- [36] S.-H. Chong and M. Fuchs, Phys. Rev. Lett. **88**, 185702 (2002).
- [37] E. del Gado, L. De Arcangelis and A. Coniglio, in preparation (2002).
- [38] We note that this value is slightly higher than the one observed in Fig. 11(b), because we are here looking at a

point slightly less close to the glass transition, thus localization is a bit less effective for this case. However, when this happens, it is always inside the attractive well in this part of the phase diagram.

[39] Actually, using the stretched exponential, one can fit the correlators not too badly. However, the parameters that are found from the fits are completely unreliable. Indeed, for the amplitude parameter, which should give an estimate of the non-ergodicity parameter, we find for every q -vector, the value of 1. This is the reason why we do not consider these fits to have any validity.

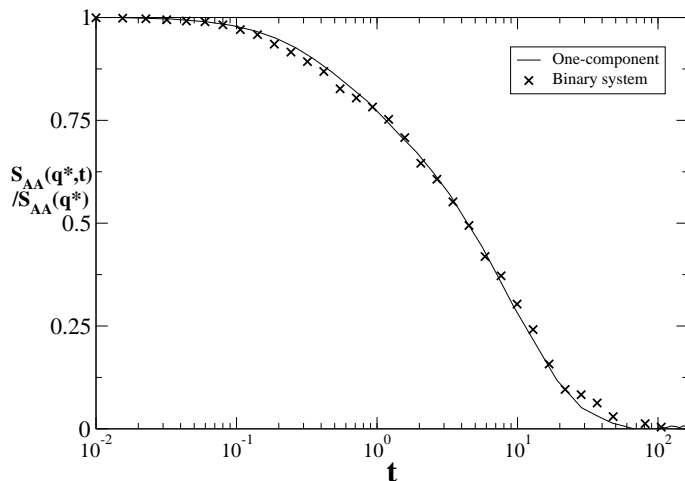


FIG. 1. Comparison between the density-density correlation function $S_{AA}(q^*, t)/S_{AA}(q^*)$ in the binary and the monodisperse case at $\phi = 0.57$ and $T = 0.75$, corresponding to the most reentrant point found in the mono-disperse case, before crystallization intervenes. The wave-vector chosen corresponds for both cases to $q^* = 2\pi/\sigma_A$.

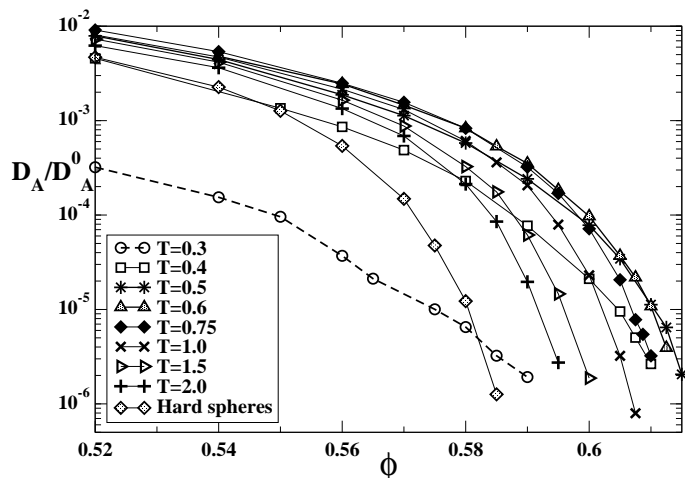


FIG. 2. Normalised diffusion constant D/D_0 , with $D_0 = \sigma\sqrt{T/m}$ in function of packing fraction ϕ , along each studied isotherms between $T = 0.3$ and $T = 2.0$. The normalisation factor takes into account the difference due to different initial velocities, and ensures the common low density limit (see [17]).

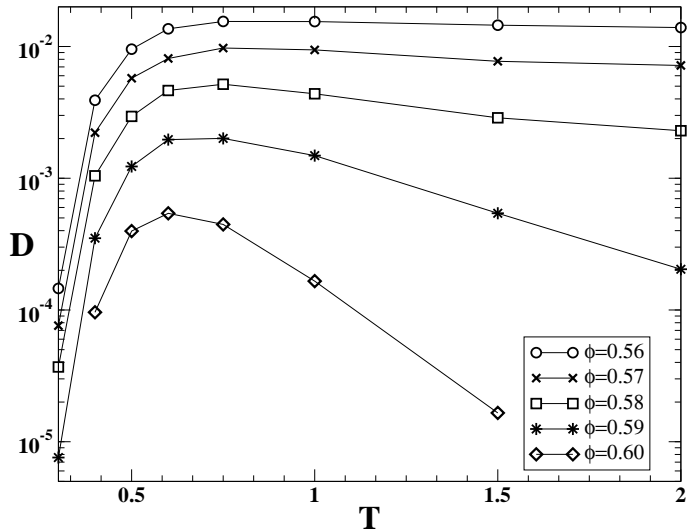


FIG. 3. As in Fig.2 but, in this case, the diffusion constant has not been normalized, and it is plotted against temperature along isochores between $\phi = 0.56$ and $\phi = 0.60$. The maximum in the bare diffusivity becomes more evident (almost 2 orders of magnitude) as one moves in the more reentrant part of the (ϕ, T) -plane.

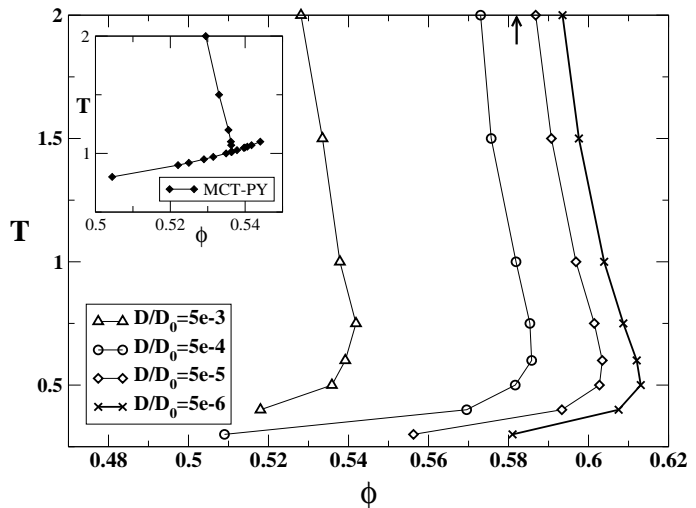


FIG. 4. Curves of iso-normalized-diffusivity D/D_0 in the (ϕ, T) plane. We indicate with a vertical arrow the location for the hard sphere case of the packing fraction ($\phi \sim 0.582$) for the lowest iso- D/D_0 curve, i.e. $D/D_0 = 5e-6$. The inset shows the MCT prediction, calculated in [4], with as input the structure factor obtained using Percus-Yevick approximation.

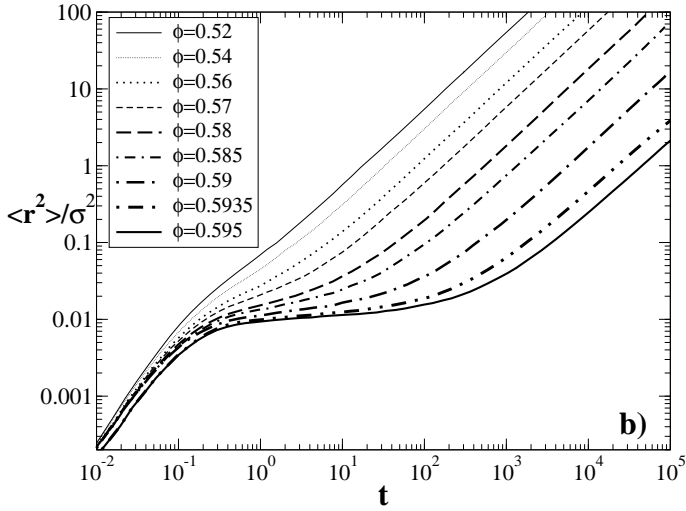
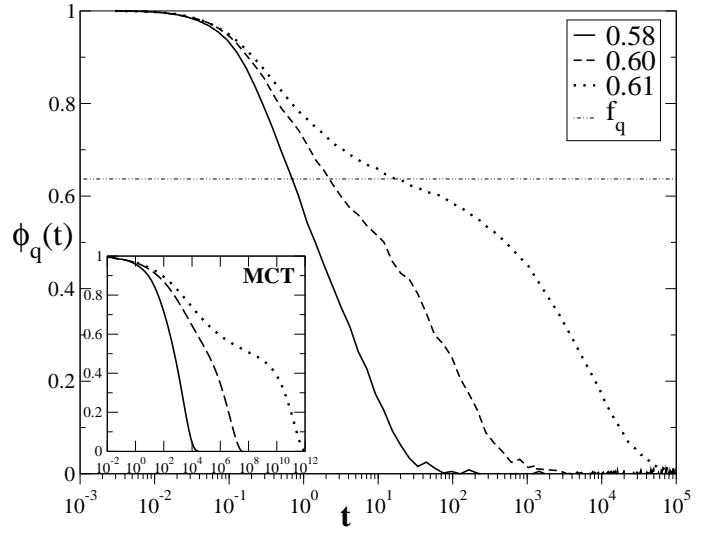
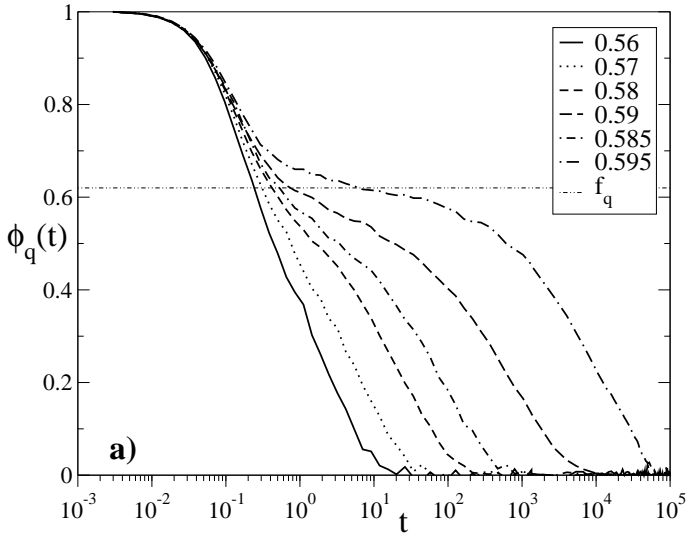


FIG. 5. a) Normalised density-density correlation function along the isotherm $T = 2.0$ for different packing fractions. The q -vector displayed in this picture is slightly larger than the one for the first peak of the static structure factor. The horizontal line represents the correspondent non-ergodicity parameter, as extrapolated from the fit (see text); b) Mean square displacement along the isotherm $T = 2.0$ for the same densities as in figures 5(a).

FIG. 6. Same as in Fig.5(a) for $T = 0.75$. The reported densities in this case have been chosen to evidence the analogy with the MCT predictions of Fig.11 in Ref. [4], reproduced in the inset for comparison.

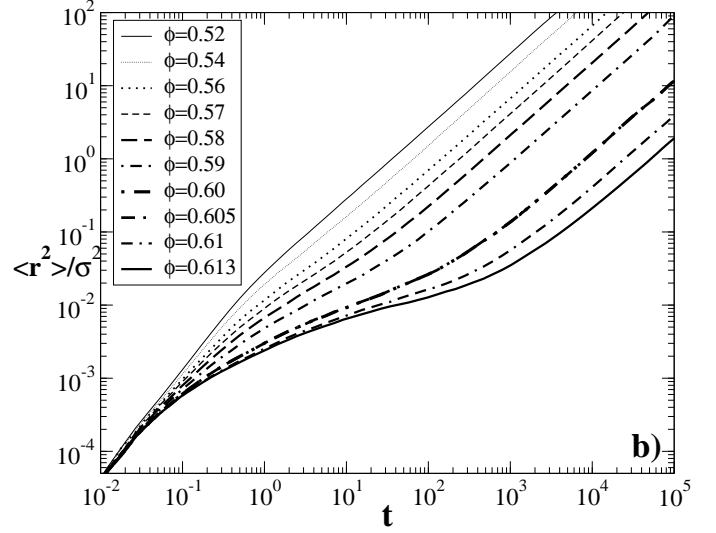
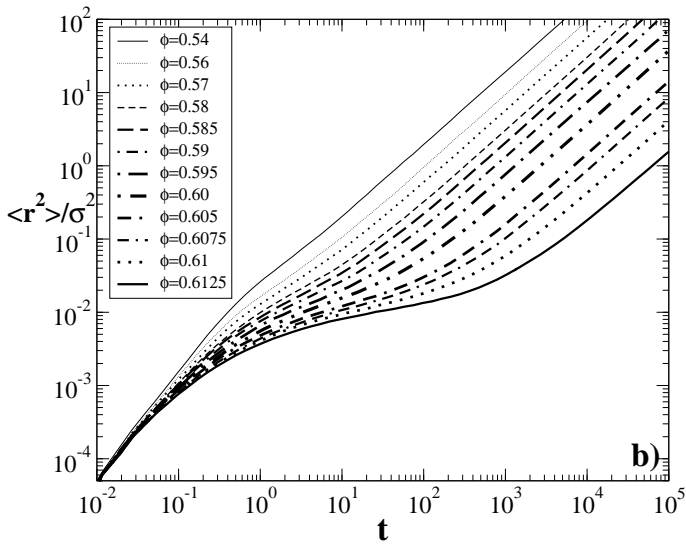
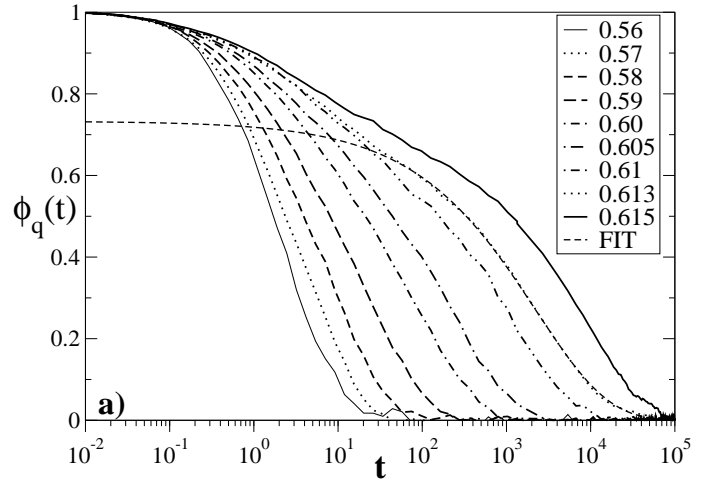
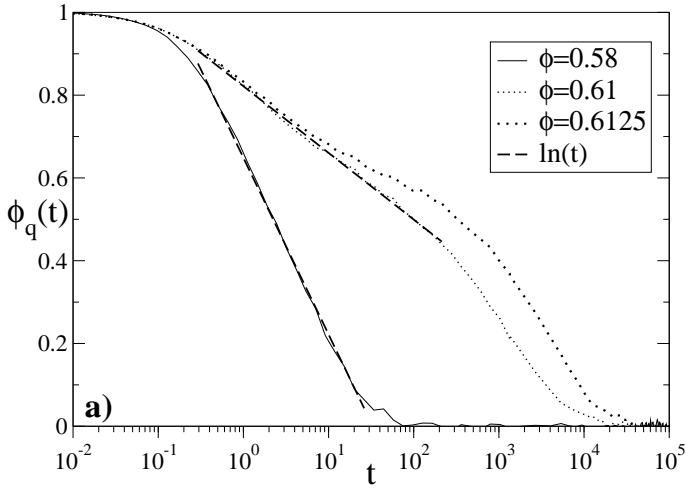


FIG. 7. a) Same as in Fig.5(a) for $T = 0.6$. The dashed lines represent fits with logarithmic laws. They are displayed to show the presence of a logarithmic decay and the mechanism of its disappearance in the proximity of an A_2 singularity (see text for further details). They are reported as a guideline to the eye, and not to extrapolate any fit parameters. b) As in Fig.5(b) for $T = 0.6$.

FIG. 8. a) As in Fig.5(a) for $T = 0.5$. The dashed line is a fit of one of the correlators with a stretched exponential, which we used to extrapolate the non-ergodicity parameter f_q , and it is shown to display the goodness of the fit. Parameters of the stretched exponential fits are reported in Fig.9. b) As in Fig.5(b) for $T = 0.5$.

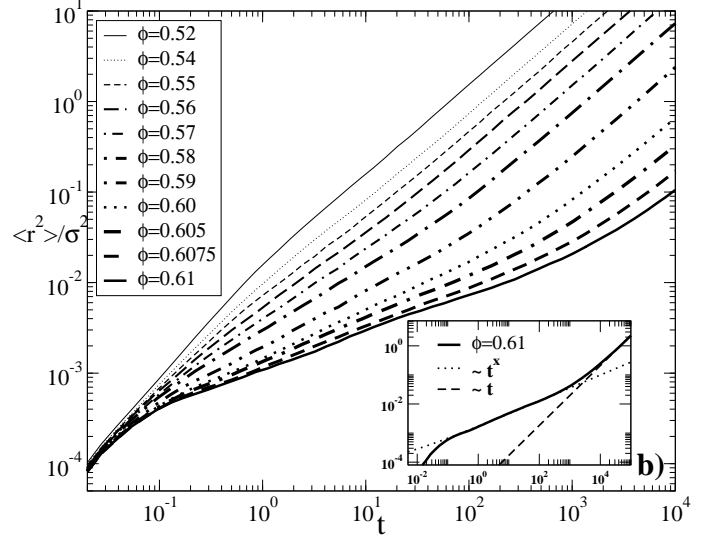
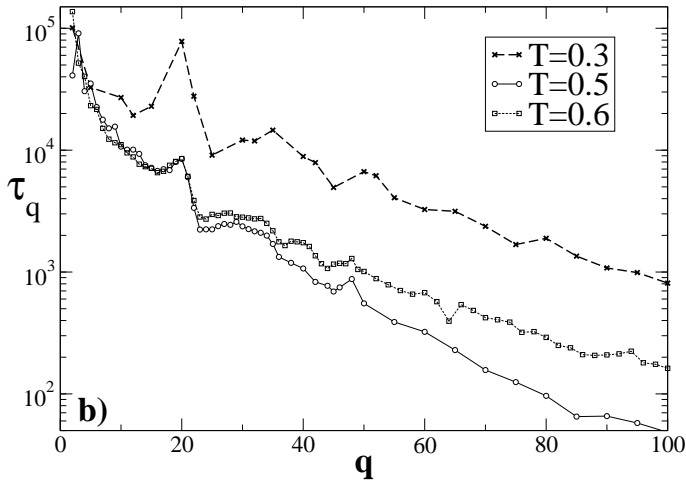
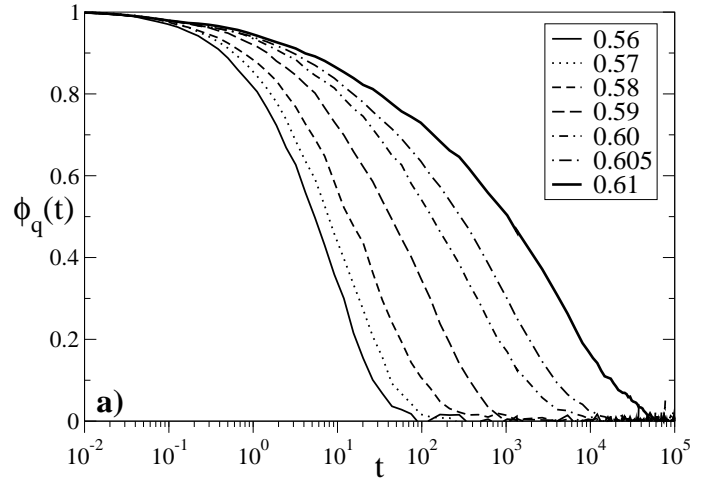
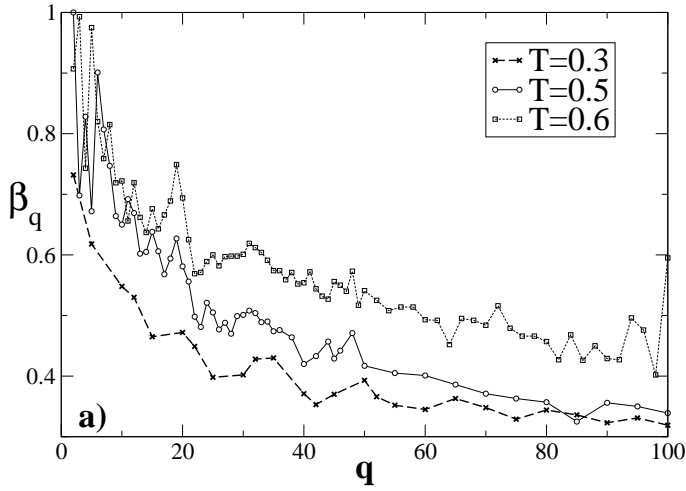


FIG. 9. a) Exponent β_q as a function of q obtained from the fit of the density-density correlation function with the stretched exponential in Eq.5 for temperatures $T = 0.6, 0.5, 0.3$. The values found are always very small, indicating a very slow relaxation. b) As in a) for the relaxation time parameter τ_q of Eq.5. Interestingly, a peak corresponding to the q -value of the static structure factor develops, as one lowers the temperature.

FIG. 10. a) As in Fig.5(a) for $T = 0.4$. b) As in Fig.5(b) for $T = 0.4$. In the inset the fit of the sub-diffusive and subdiffusive regime with a power law is shown (see text for details).

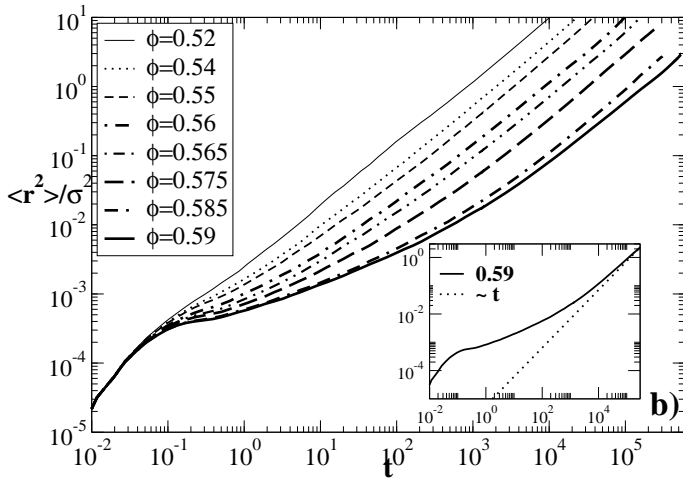
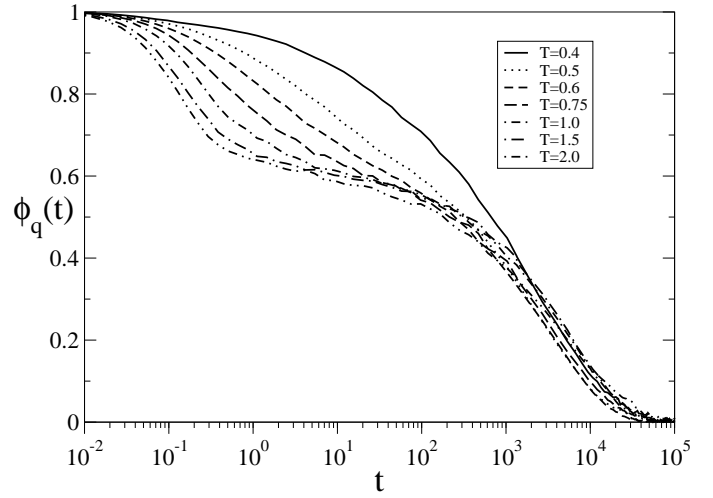
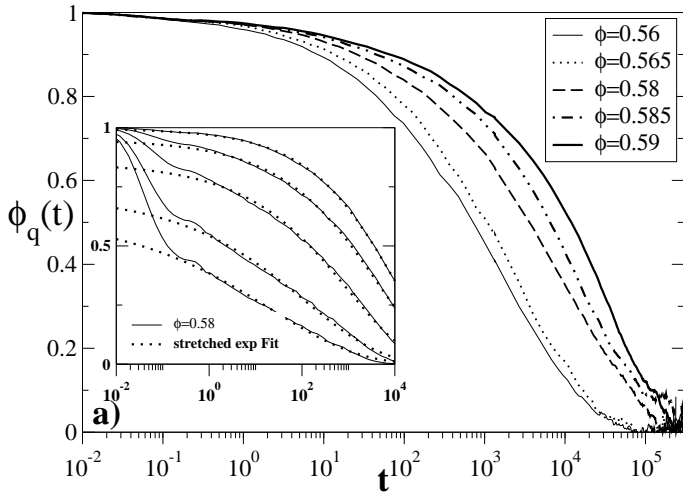


FIG. 12. Density-density correlation function along iso- D/D_0 line $D = 5 \cdot 10^{-6}$. The wave-vector chosen corresponds for all cases to $q^* = 2\pi/\sigma_A$.

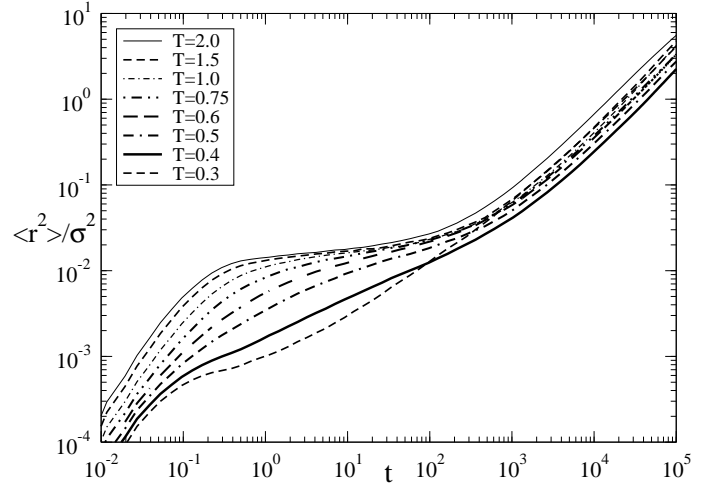


FIG. 11. a) As in Fig.5(a) for $T = 0.3$. In the inset fits with stretched exponential are shown for different value of q at the same packing fraction $\phi = 0.58$. b) As in Fig.5(b) for $T = 0.3$. In the inset a fit as in Fig.10(b) is shown. There is no evident subdiffusive regime.

FIG. 13. Mean square displacement along iso- D/D_0 line $D = 5 \cdot 10^{-6}$.

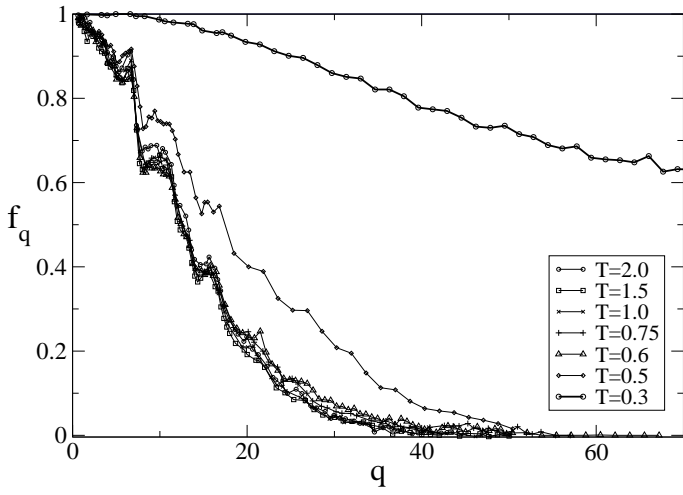


FIG. 14. Non ergodicity parameter f_q along iso- D/D_0 line $D = 5 \cdot 10^{-6}$ as obtained by fitting the correlation functions (see text for details).

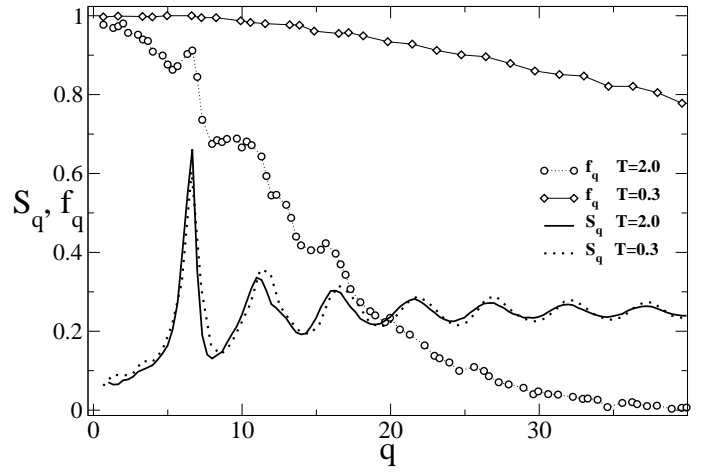


FIG. 15. Non ergodicity parameter f_q and partial static structure factor S_q at $T = 2.0$ and $T = 0.3$. The different shape of f_q reflects the difference between attractive and repulsive glass (see text for details).